

# RECENT PROGRESS ON THE COMMISSIONING OF A GAS CURTAIN BEAM PROFILE MONITOR USING BEAM INDUCED FLUORESCENCE FOR HIGH LUMINOSITY LHC

M. Ady, O. R. Jones, S. Mazzoni<sup>†</sup>, I. Papazoglou, C. Pasquino, A. Rossi,  
S. Sadovich, G. Schneider, R. Veness, CERN, Geneva, Switzerland  
P. Forck, S. Udrea, GSI, Darmstadt, Germany  
N. Kumar, A. Salehilashkajani, C. P. Welsch, H. D. Zhang  
University of Liverpool and Cockcroft Institute, Warrington, UK

## Abstract

For the high-luminosity upgrade of the Large Hadron Collider (“HL-LHC”), active control of proton beam halo will be essential for safe and reliable operation. Hollow Electron Lenses can provide such active control by enhancing the depletion of halo particles, and are now an integral part of the high luminosity LHC collimation system. The centring of the proton beam within the hollow electron beam will be monitored through imaging the fluorescence from a curtain of supersonic gas. In this contribution we report on the recent progress with this monitor and its subsystems, including the development of an LHC compatible gas-jet injection system, the fluorescence imaging setup and preliminary test measurement in the LHC.

## INTRODUCTION

The high-luminosity upgrade of the Large Hadron Collider (“HL-LHC”) is a major upgrade of LHC that aims at extending its operability by a decade by increasing its instantaneous luminosity by a factor five beyond its present design value [1]. At the core of the HL-LHC is the upgrade of the focusing triplets to allow for a smaller  $\beta^*$  in the interaction region, combined with compact superconducting radio frequency crab cavities for bunch rotation. These are advanced technical solutions that require a substantial modification of a number of LHC subsystems. The collimation system for HL-LHC, for instance, will require an improved cleaning performance to cope with the increased stored beam energy. To achieve this, is it envisaged to control the diffusion of halo particles by means of a Hollow Electron Lens (HEL) [2]. This will enclose the circulating proton beam with a low energy electron beam, deflecting any halo protons that drift into the electron beam, while leaving the proton beam core unaffected. Key to a correct operation of the HEL is the centring of the circulating proton beam within the hollow electron beam to guarantee that the core will propagate in a region of negligible electromagnetic field. To monitor the HEL alignment, a beam gas curtain (BGC) profile monitor using fluorescence is under development in the framework of the HL-LHC project through a collaborative effort between CERN, GSI and the Cockcroft Institute / University of Liverpool. In this contribution we report on recent progress with the development of the

BGC and its subsystems and on the installation of a prototype that will be operated during the next LHC physics run.

## BGC PRELIMINARY STUDIES

### Beam Gas Curtain Models and Simulations

Gas curtain generation in the BGC consists of several stages between the gas injection point and the beam interaction chamber. These stages are separated by skimmers, selecting only the central, co-linear part of the gas jet while rejecting the rest. The resulting pressure drop is approximately 2 orders of magnitude per stage. The Monte Carlo code Molflow+ was used to simulate the pressure distribution after the final skimmer, assuming a free molecular flow regime after the first skimmer. Skimmer sizes were therefore calculated so that the expanding gas curtain achieves a width of 20 mm at the interaction point, which is sufficiently wide to cover the hollow electron beam and allow a margin for beam position changes.

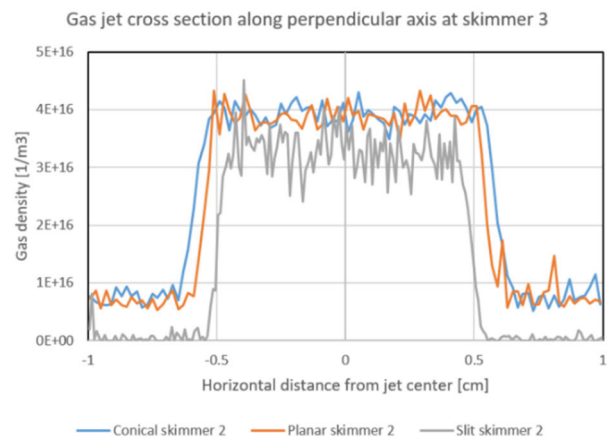


Figure 1: Density profiles for different second skimmer shapes before the interaction point.

Given the skimmer positions (determined by mechanical constraints) and the required sizes, a series of simulations were carried out to verify the gas density in the system to optimize the density within the jet and low contaminations outside of the stream. Figure 1 shows the density profiles at skimmer 3 for different second skimmer shapes before the interaction point. The planar con-

Content from this work may be used under the terms of the CC BY 3.0 licence (© 2020). Any distribution of this work must maintain attribution to the author(s), title of the work, publisher, and DOI

figuration is seen to perform the best and is the one chosen for the LHC prototype instrument.

One of the factors which may limit the spatial resolution of the BGC beam diagnostics set-up is the thickness of the gas curtain. To estimate its influence, a simplified 2D model was developed, with the assumption that the curtain is considered to have a lateral extension much larger than the beam under investigation and the same gas density throughout the width of the curtain. Since the gas density is very low, the refractive index of the curtain can be considered equal to that of vacuum (i.e.  $n_c = 1$ ). The charged particle beam has radial symmetry, which in 2D means that its flux depends only on the distance from the beam axis. Background gas density is neglected, since it is homogeneously distributed and therefore has no contribution to the shape of the profile. Finally, ideal optics with a practically infinite depth of field is assumed and the detector has just one dimension. Under these conditions the detected intensity profile can be calculated (see [3] and references therein).

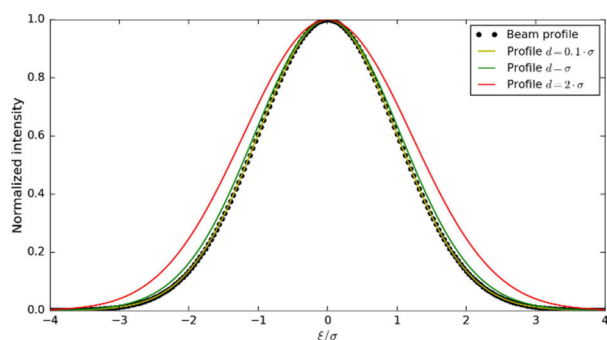


Figure 2: Recorded profiles estimated based on the present 2D model as a function of the curtain thickness  $d$ .

When considering a charged particle beam with a Gaussian transverse profile of RMS width  $\sigma$ , and a curtain with parabolic density distribution, the observed profiles are presented in Fig. 2 for curtain thicknesses  $d = 0.1 \cdot \sigma$ ,  $\sigma$ , and  $2 \cdot \sigma$ . At  $d = 2 \cdot \sigma$  the increase of the profile width in the image is clearly visible, with the observed RMS width  $\approx 1.2 \cdot \sigma$ . According to this model, the profile is expected to be reproduced with relatively good accuracy if  $d$  is kept below  $2 \cdot \sigma$ . However, if increasing the signal strength is of a higher priority one has to consider that signal amplitude saturation occurs due to the recorded profile's FWHM increasing with the curtain's thickness. The model shows that curtain thicknesses beyond  $d \approx 5 \cdot \sigma$  bring no benefit in terms of signal strength.

### Electron Beam Measurements with the BGC Lab Model

A laboratory model of the BGC is installed at the Cockcroft Institute, UK, and is shown in Fig. 3. The instrument can generate a gas curtain with a density around  $\sim 10^{16}$  molecules/ $m^3$  within a size of  $8 \times 1.5$  mm<sup>2</sup>. Because of the differential pumping, the pressure in the interaction chamber maintained at  $\sim 10^{-9}$  mbar even with a highly outgassing electron gun nearby. The profile of a 5 keV

electron beam was recently measured using Nitrogen (N<sub>2</sub>), Neon (Ne) and Argon (Ar) gas where the wavelengths of the fluorescence photons are centred at 391.4 nm, 585.4 nm and 476.5 nm respectively. A photon-counting method was used to create the image from the fluorescence generated from the gas-beam interaction.

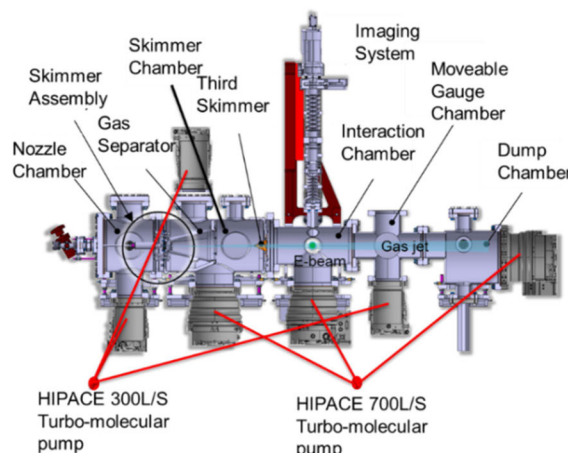


Figure 3: Schematic view of the prototype BGC monitor at the Cockcroft Institute.

Unlike N<sub>2</sub>, the wavelength of the fluorescent photons emitted from both Ne and Ar are in the same range of the spectrum as the electron gun filament emissions. This leads to an increase in background noise for these gases which is hard to remove even by using a narrow bandpass filter around the wavelength of interest. A small, blackened aluminium foil with an opening diameter of 3 mm was therefore placed between the electron gun and the interaction region in the vacuum to reduce the filament light. A set of background measurements was also taken with no gas-curtain present to allow this background to be subtracted from the data. The normalised intensity plots of nitrogen, neon and argon are displayed in Fig. 4, showing a good agreement between the three profiles.

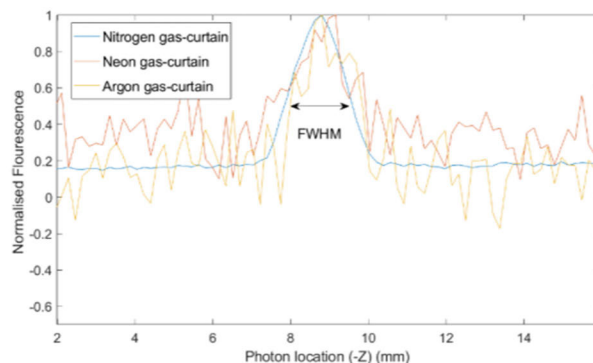


Figure 4: Normalised intensity plots of nitrogen (400 s integration time), neon and argon (4000 s integration time).

The photon detection rate is approximately 10 times lower for Ar and Ne when compared to N<sub>2</sub> under similar conditions. This is due to their smaller cross-sections and,

Content from this work may be used under the terms of the CC BY 3.0 licence (© 2020). Any distribution of this work must maintain attribution to the author(s), title of the work, publisher, and DOI

for Ne, also lower photo-cathode efficiency, which is compensated somewhat by a higher gas curtain density. The number of photons detected can be estimated [4] for each gas to the correct order of magnitude based on gas curtain density, cross section, e-beam current and optical properties. A comparison between the theoretical estimations and the measured photon number shows a reasonable agreement, as shown in Table 1. For both the HEL expected photons and lab conditions the gas-curtain density is assumed to be  $2.5 \times 10^{-16} \text{ m}^{-3}$ . The e-beam used in lab conditions has a current of 0.65 mA and 5 KeV energy. The lower measured photon with respect to the estimated one can be explained by a lower than expected gas-curtain density, especially in the case of Nitrogen, overestimation of the solid angle or optics transmission or photon losses in the intensifier. Scaling this to the properties of the future device foreseen for the electron lens, the expected photon rate will be at least 4 orders of magnitude higher, reducing the required integration time to obtain correct image to below the second.

Table 1: Comparison of the Fluorescence Photon Rate (in Counts/s) for Different Working Gases for the Prototype BGC Monitor and the Final Electron Lens BGC Monitor

Emitter	HEL expected	Lab conditions	Measured
N <sub>2</sub>	$3.4 \times 10^6$	$8.8 \times 10^2$	$1.7 \times 10^1$
Ne	$2.5 \times 10^4$	6.5	1.6
Ar	$2.3 \times 10^4$	6.0	1.3

### LHC Fluorescence Tests

Beam profile measurements based on fluorescence in the CERN PS and SPS accelerators are reported in literature [5,6] for various gases including Ar and N<sub>2</sub>.

While these tests show promising results for beam profile reconstruction, their extrapolation to the case of the LHC is not trivial due to the significantly different beam energy. In order to quantify the S/N to be expected in the LHC, a Beam Induced Fluorescence (BIF) test instrument was installed in the course of 2018. The optical instrument is composed of two 50 mm diameter, 300 mm focal length doublets that project the image of the center plane of the beampipe onto a single micro channel plate (MCP) intensified camera with a Multialkali photocathode.

A remote controlled filter wheel allows a neutral density (ND1 – ND2) or a bandpass ( $340 \pm 40 \text{ nm}$ ,  $585 \pm 40 \text{ nm}$ ) filter to be inserted in the light path. The entire optical instrument is enclosed in a light tight container. A gas injection system allows Neon gas to be introduced inside the beam pipe up to a pressure of approximately  $5 \times 10^{-8} \text{ mbar}$ . Measurements were performed in the second half of 2018 with both protons and Pb ions, at energies from 450 Z GeV to 6.5 Z TeV. The case of Pb ions at 450 Z GeV is the one that yielded the best signal to noise, with the lowest amount of optical background. Figure 5 (a) shows the fluorescence image of Pb ions at 450 Z GeV with a very long (1286 s) exposure time. Op-

tical background and showers generated by beam loss have been subtracted from the image. The fluorescence signal appears as a streak at the very top of the image. The off-centre position of the beam with respect to the centre of the viewport is believed to be caused by a misalignment of the vacuum chamber, whose precise position with respect to the beam pipe centre was not measured before installation. Figure 5 (b) shows a Gaussian fit of the vertical profile of the fluorescence image averaged over 10 mm. The resulting width ( $\sigma = 2.2 \text{ mm}$ ) could not be directly cross-checked with another instrument as no other profile measurement device can currently measure a nominal Pb ion beam at injection energy. It is possible however to deduce that the average transverse beam size could not have been greater than 2.1 mm. This is derived from the measurement of the beam size at high energy as performed by the Beam Synchrotron Radiation Telescope (BSRT) and rescaled to an energy of 450 Z GeV assuming no emittance growth during the energy ramp. The fluorescence measurement is therefore consistent with such a value. However, further studies are clearly needed to better characterize the accuracy, as the measurement of the LHC beam profile was not the main goal of the test.

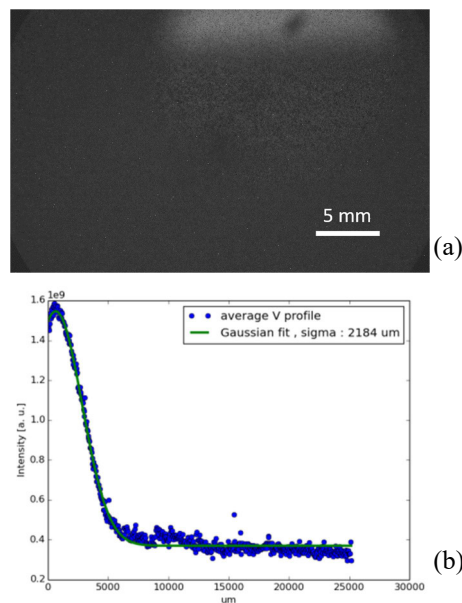


Figure 5: Top: Fluorescence image of Pb ions at 450 Z GeV with an integration time of 1286 s and the optical background subtracted. The black mark is due to a defect of the photocathode. Bottom: Fit of the vertical profile averaged longitudinally over 10 mm.

When reducing integration time, the BIF setup allows us to measure the evolution of the beam profile as a function of time, as shown in Fig. 6 where integration time was set to 40 seconds. The measurement was performed during the filling of the LHC, with a circulating charge ranging from  $2 \times 10^{12} \text{ C}$  to  $1.2 \times 10^{13} \text{ C}$ . Data points before 18:40:00 (hh:mm:ss) are to be discarded as the stored beam current was too low for the selected exposure time.

Measurements with Pb ions at high energy and with protons at both injection and high energy are inconclusive

due to an insufficient signal to noise ratio. For the particular case of protons at high energy (the relevant case for HEL alignment), the main source of noise is suspected to be synchrotron radiation reflected from the copper beam pipe surface opposite to the viewport. This results in a background  $10^4$  times higher than the one measured for the Pb ions at injection. This test therefore highlighted the importance of a reducing any parasitic reflection from entering the imaging optics by means of proper coating for absorption.

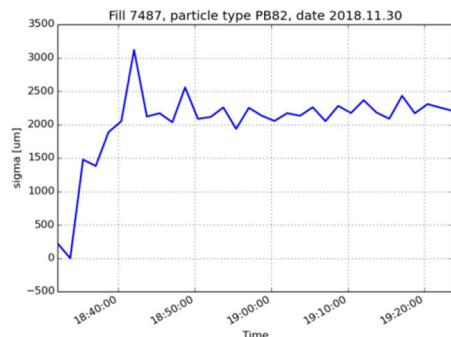


Figure 6: Beam size ( $\sigma$ ) as a function of time for Pb ions beam. Integration time is 40 s.

## INSTALLATION OF BGC PROTOTYPE IN THE LHC

A BGC prototype has been designed and is currently being built. The installation of the demonstrator instrument will happen in two phases. The first phase, now installed, includes the main gas curtain interaction chamber, a simple gas injection system and the optical instrument used for previous fluorescence measurements. In order to minimise optical background the entire vacuum chamber is blackened with amorphous carbon coating (see Fig. 7), while in front of the camera, a specially designed plate is inserted with a vacuum compatible, multilayer coating to give a reflectivity of 0.2-0.5% at the wavelength of interest (585.4 nm). By applying these coatings, the optical background reaching the camera should be sufficiently reduced to allow imaging at high energy with protons. In phase 2 the full BGC instrument will be installed, including the supersonic gas curtain generation and the final optical system (see Fig. 8). The selected working gas is injected at a pressure of 10 bar through a 30 mm nozzle. The jet is then shaped with a series of 3 skimmers, resulting in a final equivalent pressure in the  $10^{-7}$  mbar range (corresponding to a density of  $2.47 \times 10^9 \text{ cm}^{-3}$ ) while the background pressure is expected to be in the  $10^{-9}$  mbar range. A gas dump system is placed on the opposite side of the gas injection system in order to collect the gas curtain after the beam interaction to maintain as low as possible a background pressure in the interaction chamber. A slit aperture matching the gas curtain dimensions is placed at the entrance to the dump chamber, which allows the gas jet to enter but prevents the majority of any reflected gas from re-entering the interaction volume.

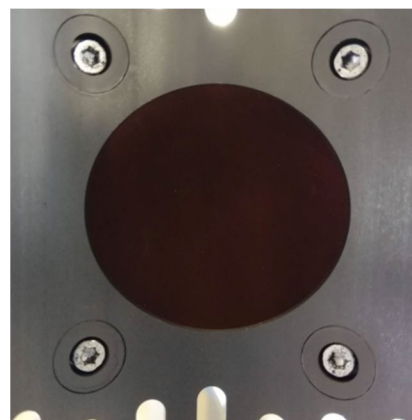


Figure 7: Amorphous carbon coating together with the multilayer coated plate.

This gas is then extracted using a high conductance pump. The gas injection system and gas dump are scheduled for testing at the Cockcroft Institute in 2020, with a subsequent test on the HEL test stand at CERN foreseen in 2021, before installation in the LHC.

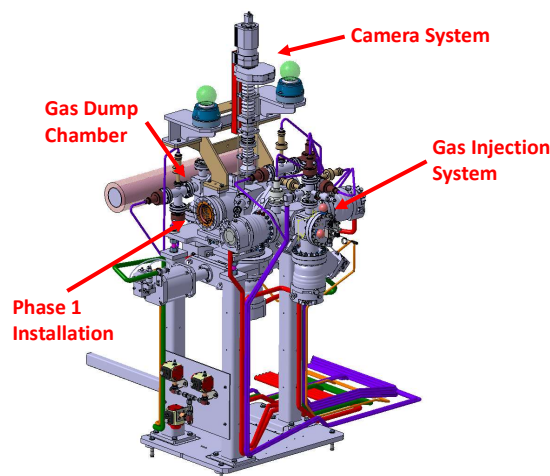


Figure 8: Phase 2 of the final BGC demonstrator.

## SUMMARY

We have presented the recent progress of the BGC development, including simulation and analysis of the gas curtain shaping, fluorescence measurements of 5 keV electrons in the laboratory and of Pb ions in the LHC. A BGC demonstrator has been installed in the LHC with blackened vacuum chamber surfaces for improved optical background reduction. The BGC demonstrator will be operated during the next LHC physics run scheduled to start in 2022.

## REFERENCES

- [1] G. Apollinari *et al.*, “High-Luminosity Large Hadron Collider (HL-LHC) Technical Design Report V. 0.1”, CERN, Geneva, Switzerland, Rep. CERN-2017-007-M, 2017.
- [2] G. Stancari, A. Valishev, G. Annala, G. Kuznetsov, V. Shiltsev, D. A. Still, and L. G. Vorobiev, “Collimation with Hollow Electron Beams”, *Phys. Rev. Lett.*, vol. 107, p. 084802, 2011. doi: 10.1103/PhysRevLett.107.084802

Content from this work may be used under the terms of the CC BY 3.0 licence (© 2020). Any distribution of this work must maintain attribution to the author(s), title of the work, publisher, and DOI

- [3] S. Udrea and P. Forck, “CERN e-lens Milestone 1.6 report v2”, Rep. CERN EDMS 2333413, Sept. 2018.
- [4] R. Veness *et al.*, “Development of a Beam-Gas Curtain Profile Monitor for the High Luminosity Upgrade of the LHC”, in *Proc. IBIC'18*, Shanghai, China, Sep. 2018, pp. 472-476. doi:10.18429/JACoW-IBIC2018-WEPB16
- [5] M. A. Plum, E. Bravin, J. Bosser, and R. Maccaferri, “N2 and Xe gas scintillation cross-section, spectrum, and lifetime measurements from 50 MeV to 25 GeV at the CERN PS and Booster”, *Nucl. Instrum. Methods in Phys. Res. A*, vol. 492, pp. 74–80, 2002. doi: 10.1016/S0168-9002(02)01287-1
- [6] A. Variola, R. Jung, and G. Ferioli, “Characterization of a nondestructive beam profile monitor using luminescent emission”, *Phys. Rev. ST Accel. Beams*, vol. 10, p. 122801, 2007. doi: 10.1103/PhysRevSTAB.10.122801
- [7] J. Glutting, “Blackening Investigation for the BGC Interaction Chamber”, Rep. CERN EDMS 2052543, Dec. 2018.